

Search for exclusive events using the dijet mass fraction at the Fermilab Tevatron

O. Kepka*

DAPNIA/Service de physique des particules, CEA/Saclay, 91191 Gif-sur-Yvette cedex, France
IPNP, Faculty of Mathematics and Physics, Charles University, Prague
and Center for Particle Physics, Institute of Physics, Academy of Science, Prague

C. Royon†

DAPNIA/Service de physique des particules, CEA/Saclay, 91191 Gif-sur-Yvette cedex, France
 (Received 11 April 2007; published 21 August 2007)

In this paper, we discuss the observation of exclusive events using the dijet mass fraction as measured by the CDF Collaboration at the Fermilab Tevatron. We compare the data to Pomeron exchange inspired models as well as soft color interaction ones. We also provide the prediction on the dijet mass fraction at the CERN LHC using both exclusive and inclusive diffractive events.

DOI: [10.1103/PhysRevD.76.034012](https://doi.org/10.1103/PhysRevD.76.034012)

PACS numbers: 13.85.Hd

I. INTRODUCTION

Double Pomeron exchange (DPE) processes are expected to extend the physics program at the CERN LHC not only due to the possible Higgs boson detection but also because of the possibility to study a broader range of QCD physics and diffraction [1–8]. The processes are theoretically characterized by large rapidity gap regions devoid of particles between a centrally produced heavy object and the scattered hadrons which leave the interaction intact. This is attributed to the exchange of a colorless object, the Pomeron (or the Reggeon). In the LHC environment, however, the rapidity gap signature will not appear because of the high number of multiple interactions occurring at the same time, and the diffractive events will be identified by tagging the escaping protons in the beam pipe.

One generally considers two classes of DPE processes, namely, *exclusive* DPE events if the central object is produced alone carrying away the total available diffractive energy, and *inclusive* events when the total energy is used to produce the central object and, in addition, the Pomeron remnants. Exclusive events allow a precise reconstruction of the mass and kinematical properties of the central object using the central detector or even more precisely using very forward detectors installed far downstream from the interaction point. The most appealing exclusive process to be studied at the LHC is the Higgs boson production, but since it cannot be observed at the Fermilab Tevatron due to the low production cross section, one should find other ways to look for exclusive events at the Tevatron, for example, in dijet, diphoton channels. It is necessary to mention that, until recently, there was not a decisive measurement that would provide enough evidence for the existence of exclusive production.

Although exclusive production yields kinematically well-constrained final state objects, their experimental de-

tection is nontrivial due to the overlap with the *inclusive* DPE events. In those events, the colliding Pomerons are usually viewed as an object with partonic substructure. A parton emitted from the Pomeron takes part in the hard interaction, and Pomeron remnants accompanying the central object are distributed uniformly in rapidity. Exclusive events usually appear as a small deviation from the inclusive model predictions which need to be studied precisely before accepting a new kind of production. In particular, the structure of the Pomeron as obtained from HERA is not precisely known at a high momentum fraction, and, specifically, the gluon in the Pomeron is not well constrained. It is not clear if such uncertainty could not lead to misidentifying observed processes as exclusive. This would, for instance, preclude the spin analysis of the produced object.

In this paper, we aim to investigate the observation of exclusive production at the Tevatron. Indeed, we use the dijet mass fraction (DMF) distribution measured by the CDF Collaboration and show that, even when taking into account uncertainties associated with the Pomeron structure, one is unable to give a satisfactory description of the data without the existence of exclusive events. We also include another approach to explain diffraction in our study, the so-called soft color interaction (SCI) model (the properties of all the models are discussed later). As an outlook, we apply current models for the DPE production for LHC energies and demonstrate the possible appearance of exclusive events through the dijet mass fraction.

The paper is organized as follows: in Sec. II we give a brief description of the inclusive, exclusive, and soft color interaction models. Section III discusses how well the various models can explain the preliminary Tevatron dijet mass fraction data and the constraints implied by the data on the current models. In Sec. IV, we foreshadow an application of the dijet mass fraction distribution as a tool to observe exclusive events at LHC energies. Finally, we discuss issues concerning the dijet mass fraction

*kepkao@fzu.cz

†royon@hep.saclay.cea.fr

reconstruction and fast detector simulation in the Appendix.

II. THEORETICAL MODELS

Inclusive and exclusive DPE models used in this paper are implemented in the Monte Carlo program DPEMC [9]. The soft color interaction model is embedded in the PYTHIA program [10]. The survey of the different models follows.

A. Inclusive models

The first inclusive model to be mentioned is the so-called “factorized model” (FM). It is an Ingelman-Schlein type of model [11] describing the diffractive double Pomeron process as a scattering of two Pomerons emitted from the proton, assuming a factorization of the cross section into a Regge flux convoluted with the Pomeron structure functions. For ep single diffraction, it is necessary to introduce a secondary Reggeon trajectory to describe the observed single diffractive nonfactorable cross section. In the case of the Tevatron, the Pomeron trajectory alone is sufficient to describe present data and the cross section is factorable as it was advocated in [12]. Factorization breaking between HERA and Tevatron comes only through the survival probability factor, denoting the probability that there is no additional soft interaction which would destroy the diffractively scattered protons. In other words, the probability to destroy the rapidity gap does not depend on the hard interaction. At Tevatron energies, the factor was measured to be approximately 0.1, and calculation suggested the value of 0.03 for the LHC. Pomeron structure functions, and Reggeon and Pomeron fluxes are determined from the deep inelastic scattering ep collisions fitting the diffractive structure function F_2^D at HERA. For one of the most recently published diffractive structure function analyses, see e.g. [13].

On the other hand, the Boonekamp-Peschanski-Royon (BPR) inclusive model [8] is a purely nonperturbative calculation utilizing only the shape of the Pomeron structure function and leaving the overall normalization to be determined from the experiment; one can, for example, confront the prediction of the DPE cross section with the observed rate at the Tevatron [12] and obtain the missing normalization factor.¹

Both models use the Pomeron structure measured at HERA which is gluon dominated. In this paper, we use the results of the QCD fits to the most recent Pomeron

structure function data measured by the H1 Collaboration [13]. The new gluon density in the Pomeron is found to be slightly smaller than the previous one, and it is interesting to see the effect of the new PDFs with respect to the Tevatron measurements. Moreover, the gluon density at high β , where β denotes the fraction of the particular parton in the Pomeron, is not well constrained by the QCD fits performed at HERA. To study this uncertainty, we multiply the gluon distribution by the factor $(1 - \beta)^\nu$ as shown in Fig. 1. QCD fits to the H1 data lead to the uncertainty on the ν parameter $\nu = 0.0 \pm 0.5$ [13]. We will see in the following how this parameter influences the results on the dijet mass fraction as measured at the Tevatron.

B. Exclusive models

The Bialas-Landshoff (BL) exclusive model [14] is based on an exchange of two “nonperturbative” gluons between a pair of colliding hadrons which connect to the hard subprocess. Reggeization is employed in order to recover the Pomeron parameters which successfully described soft diffractive phenomena, e.g. the total cross section at low energies. It should be mentioned that the so-called Bialas-Landshoff exclusive model is actually an extension of the Higgs boson exclusive production calculated by Bialas and Landshoff (see first reference of [14]) for the dijet production. This is composed of a cross section for $q\bar{q}$ production [14] obtained by Bialas, Szeremeta, and Janik, and for gg production performed by Bzdak [15].

On the contrary, the Khoze, Martin, Ryskin (KMR) [16] model is purely a perturbative approach. The interaction is obtained by an exchange of two gluons directly coupled to the colliding hadrons (no Pomeron picture is introduced). While one gluon takes part in the creation of the central object, the other serves to screen the color flow across the rapidity gap. If the outgoing protons remain intact and scatter at small angles, the exchanged di-gluon system, in both models, must obey the selection rules $J_Z = 0$, C-even, P-even. Such constraints are also applied to the hard subprocesses for the production of the central object.

The two models show a completely different p_T dependence of the DPE cross section. The energy dependence of the BL model is found to be weaker since the Pomeron is assumed to be soft, whereas this is not the case for the KMR model.

C. Soft color interaction model

The SCI model [10,17] assumes that diffraction is not due to a colorless exchange at the hard vertex but rather to a string rearrangement in the final state during hadronization. This model gives a probability (to be determined by experiment) that there is no string connection, and so no color exchange, between the partons in the proton and the scattered quark produced during the hard interaction. Since the model does not imply the existence of a Pomeron, there

¹One more remark is in order. In the BPR model, the partonic content of the Pomeron is expressed in terms of the distribution functions as $f_{i/\mathbb{P}}(\beta_i) \equiv \beta_i G_{i/\mathbb{P}}(\beta_i)$, where $G_{i/\mathbb{P}}(\beta_i)$ are the true parton densities as measured by the HERA Collaboration, and β_i denotes the momentum fraction of the parton i in the Pomeron. The integral of $f_{i/\mathbb{P}}(\beta_i)$ is normalized to 1, so that in the limit $f_{i/\mathbb{P}}(\beta_i) \rightarrow \delta(\beta_i)$ the exclusive cross section of the Bialas-Landshoff model is recovered [9].

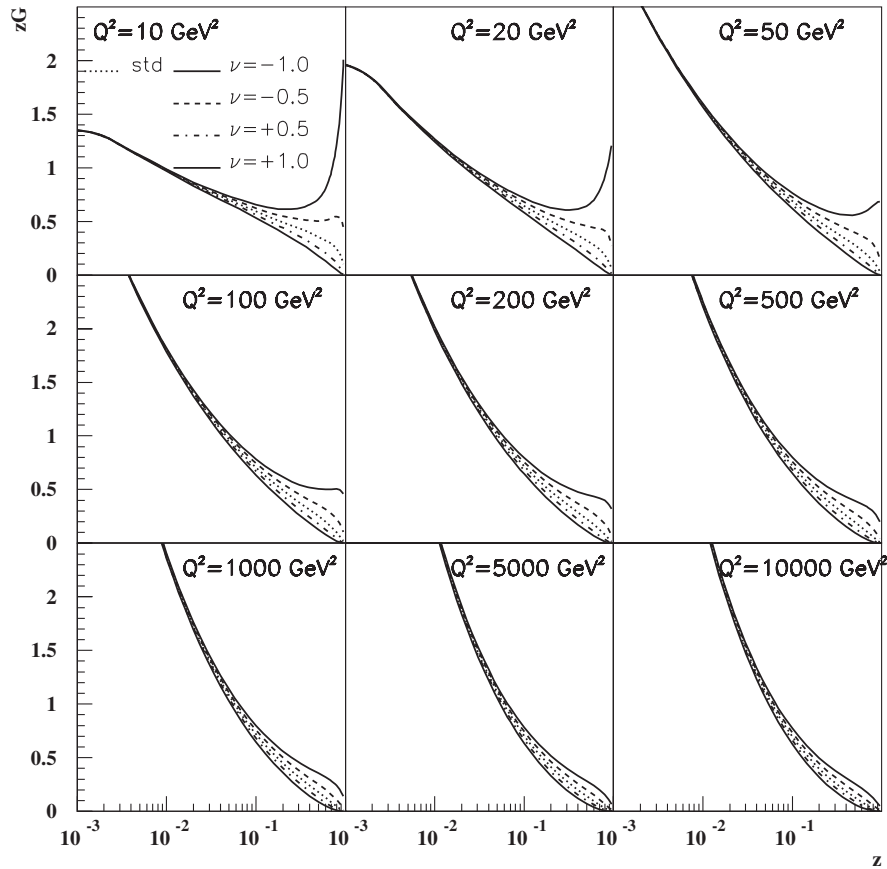


FIG. 1. Uncertainty of the gluon density at high β (here $\beta \equiv z$). The gluon density is multiplied by the factor $(1 - \beta)^\nu$ where $\nu = -1, -0.5, 0.5, 1$. The default value $\nu = 0$ is the gluon density in the Pomeron determined directly by a fit to the H1 F_2^D data with an uncertainty of about 0.5.

is no need for a concept like survival probability and a correct normalization is found between single diffraction Tevatron and HERA data without any new parameter, which is one of the big successes of this model.

III. DIJET MASS FRACTION AT THE TEVATRON

The DMF turns out to be a very appropriate observable for identifying the exclusive production. It is defined as a ratio $R_{JJ} = M_{JJ}/M_X$ of the dijet system invariant mass M_{JJ} to the total mass of the final state system M_X (excluding the intact beam (anti)protons). If the jet algorithm has such properties that the outside-cone effects are small, the presence of an exclusive production would manifest itself as an excess of the events towards $R_{JJ} \sim 1$; for exclusive events, the dijet mass is essentially equal to the mass of the central system because no Pomeron remnant is present. The advantage of the DMF is that one can focus on the shape of the distribution; the observation of exclusive events does not rely on the overall normalization which might be strongly dependent on the detector simulation and acceptance of the roman pot detector.

In the following analysis, we closely follow the measurement performed by the CDF Collaboration. One can

find more information about the measurement and the detector setup in a note discussing preliminary results [18]. In this paragraph, we will mention only the different cuts which are relevant for our analysis. To simulate the CDF detector, we use a fast simulation interface [19], which performs a smearing of the deposited cell energy above a 0.5 GeV threshold and reconstructs jets using a cone algorithm. Properties of the event such as the rapidity gap size were evaluated at the generator particle level.

CDF uses a roman pot detector to tag the antiprotons on one side (corresponding to $\eta_{\bar{p}} < 0$). For the DMF reconstruction, we require the antiprotons to have the longitudinal momentum loss in the range $0.01 < \xi_{\bar{p}} < 0.12$, and we apply the roman pot acceptance obtained from the CDF Collaboration (the real acceptance is greater than 0.5 for $0.035 < \xi_{\bar{p}} < 0.095$). On the proton side, where no such device is present, a rapidity gap of the size $3.6 < \eta_{\text{gap}} < 5.9$ is required. In the analysis, further cuts are applied: two leading jets with a transverse momentum above the threshold $p_T^{\text{jet1,jet2}} > 10$ GeV or $p_T^{\text{jet1,jet2}} > 25$ GeV in the central region $|\eta^{\text{jet1,jet2}}| < 2.5$, a third jet veto cut ($p_T^{\text{jet3}} < 5$ GeV), as well as an additional gap on the antiproton side of the size $-5.9 < \eta_{\text{gap}} < -3.6$. For the sake of brevity, the

threshold for the transverse momentum of the two leading jets will be denoted as p_T^{\min} in the following, if needed.

The dijet mass is computed using the jet momenta for all events passing the above-mentioned cuts. In order to follow as much as possible the method used by the CDF Collaboration, the mass of the diffractive system M_X is calculated from the longitudinal antiproton momentum loss $\xi_{\bar{p}}$ within the roman pot acceptance, and the longitudinal momentum loss of the proton ξ_p^{part} is determined from the particles in the central detector ($-4 < \sim \eta_{\text{part}} < \sim 4$), such that

$$M_X = \sqrt{s \xi_{\bar{p}} \xi_p^{\text{part}}}, \quad (1)$$

$$\xi_p^{\text{part}} = \frac{1}{\sqrt{s}} \sum_{\text{particles}} p_T \exp^{\eta}, \quad (2)$$

summing over the particles with energies higher than 0.5 GeV in the final state at the generator level. To reconstruct the diffractive mass, ξ_p^{part} was multiplied by a factor 1.1, obtained by fitting the correlation plot between the momentum loss of the proton at generator level ξ_p and ξ_p^{part} at particle level with a straight line.

The DMF reconstruction is deeply dependent on the accuracy of the detector simulation. Since we are unable to employ the complete simulation in our analysis, we discuss possible effects due to the various definitions of DMF on the generator level and the particle level in the Appendix.

A. Inclusive model prediction

We present first the dijet mass fraction calculated with FM and BPR models. As stated in a previous section, we want to explore the impact of the high β gluon uncertainty in the Pomeron. To do this, we multiply the gluon density by a factor $(1 - \beta)^\nu$, for diverse values of $\nu = -1, -0.5, 0, 0.5, 1$. The impact of the parameter is shown in Figs. 2 and 3 for jets with $p_T > 10$ GeV and $p_T > 25$ GeV, respectively. The computed distributions were normalized in shape, since the luminosity used for the dijet mass fraction measurement is not given. This should be understood in the following way: in the CDF note [18], the luminosity of the whole sample is given which differs from the effective luminosity used for R_{JJ} . The difference is mainly due to pileup effects. The diffractive R_{JJ} events are selected using single interactions only (gaps would be filled in by pileup interactions) which correspond on average to 1% of the whole data sample. However, the exact number is not given in the CDF note. On the other hand, one can compare the theoretical prediction to the cross section corrected to hadron level provided by CDF. We find that the cross sections agree up to a factor 2–3 for different jet p_T cuts. This difference can be attributed to the fast simulation

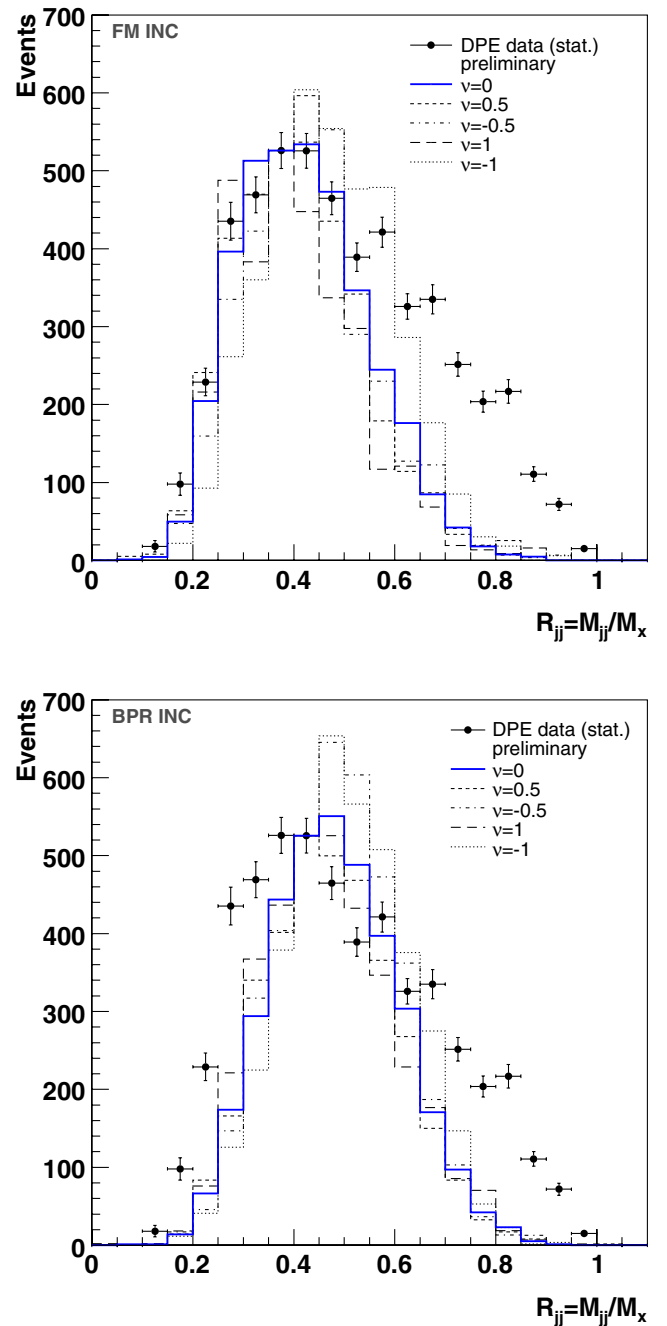


FIG. 2 (color online). Dijet mass fraction for jets $p_T > 10$ GeV. FM (top panel) and BPR (bottom panel) models, inclusive contribution. The uncertainty of the gluon density at high β is obtained by multiplying the gluon distribution by $(1 - \beta)^\nu$ for different values of ν (nonsolid lines).

which we are using. It is obvious that the size of the rapidity gap (directly related to ξ_p) is difficult to be studied without a full simulation. The factor 2–3 can be easily obtained by a small change of ξ_p since the cross section itself has $1/\xi_p$ dependence. However, it is important to notice that the shape of the dijet mass fraction does not

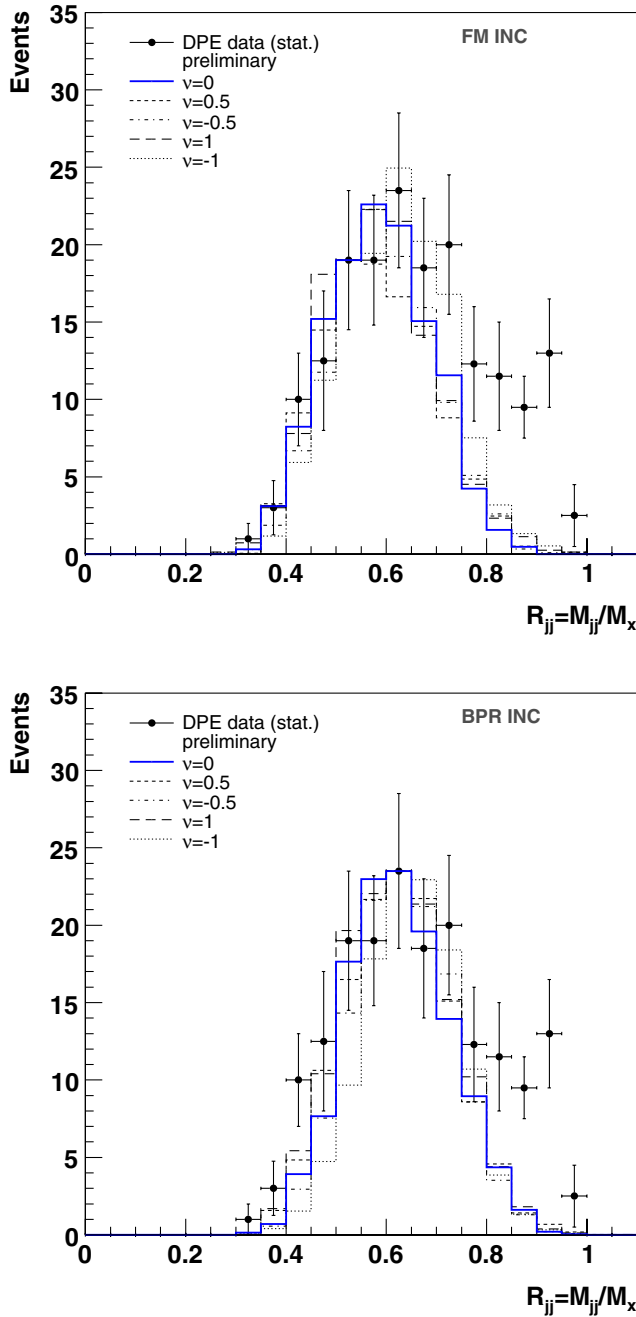


FIG. 3 (color online). Dijet mass fraction for jets $p_T > 25$ GeV. FM (top panel) and BPR (bottom panel) models, inclusive contribution. The uncertainty of the gluon density at high β is obtained by multiplying the gluon distribution by $(1 - \beta)^\nu$ for different values of ν (nonsolid lines).

TABLE I. Cross sections of inclusive diffractive production σ^{INC} , exclusive cross section σ^{EXC} to be rescaled with a relative additional normalization between inclusive and exclusive events $r^{\text{EXC/INC}}$ for $p_T > 10$ GeV and $p_T > 25$ GeV jets and for different models (see text). Note that the fit to the data is parametrized as $N(\sigma^{\text{INC}}(R_{JJ}) + r^{\text{EXC/INC}}\sigma^{\text{EXC}}(R_{JJ}))$.

Contributions	$r^{\text{EXC/INC}}(10)$	$\sigma^{\text{INC}}(10)$ [pb]	$\sigma^{\text{EXC}}(10)$ [pb]	$r^{\text{EXC/INC}}(25)$	$\sigma^{\text{INC}}(25)$ [pb]	$\sigma^{\text{EXC}}(25)$ [pb]
FM + KMR	2.50	1249	238	1.0	7.39	3.95
FM + BL EXC	0.35	1249	1950	0.038	7.39	108
BPR + BL EXC	0.46	2000	1950	0.017	40.6	108

depend strongly on ξ_p or the size of the rapidity gap as illustrated in Fig. 22, and therefore it does not change our conclusion of the description of the DMF using inclusive diffraction.

The interesting possible exclusive region at high R_{JJ} is enhanced for $\nu = -1$, but not to such an extent that would lead to a fair description of the observed distributions. As a consequence, the tail of the measured dijet mass fraction at high R_{JJ} cannot be explained by enhancing the gluon distribution at high β , and another contribution such as exclusive events is required.

A particular property seems to disfavor the BPR model at the Tevatron. Indeed, the dijet mass fraction is dumped at low values of R_{JJ} , especially for jets $p_T > 10$ GeV. Since the cross section is obtained as a convolution of the hard matrix element and the distribution functions, the dumping effect is a direct consequence of the use of a multiplicative factor β in the parton density functions in the Pomeron (see footnote ¹). We will come back to this point when we discuss the possibility of a revised version of the BPR model in the following.

As we have seen, inclusive models are not sufficient to describe the measured CDF distributions well. Thus, this opens an area to introduce different types of processes/models which give a significant contribution at high R_{JJ} .

B. Exclusive model predictions

In this section, we will study the enhancement of the dijet mass distribution using exclusive DPE processes, with the aim of describing the CDF dijet mass fraction data. We examine three possibilities of the interplay of inclusive plus exclusive contributions, specifically,

- (1) FM + KMR
- (2) FM + BL exclusive
- (3) BPR + BL exclusive

The full contribution is obtained by fitting the inclusive and exclusive distribution to the CDF data, leaving the overall normalization N and the relative normalization between the two contributions $r^{\text{EXC/INC}}$ free. More precisely, the DMF distribution is obtained with the fit as $N(\sigma^{\text{INC}}(R_{JJ}) + r^{\text{EXC/INC}}\sigma^{\text{EXC}}(R_{JJ}))$. The fit was done for jets with $p_T^{\text{min}} = 10$ GeV and $p_T^{\text{min}} = 25$ GeV, separately.

The overall normalization factor cannot be studied since the CDF Collaboration did not determine the luminosity for the DMF measurement. On the other hand, the relative

normalization between the inclusive and exclusive production is useful information. The relative normalization allows us to make predictions for higher p_T jets or for LHC energies, for instance. For this purpose, the relative normalizations $r^{\text{EXC/INC}}$ should not vary much between the two p_T^{min} measurements. Results are summarized in Table I. We give the inclusive σ^{INC} and the exclusive σ^{EXC} cross sections, obtained directly from the models, and the relative scale factor needed to describe the CDF data to be applied to the exclusive contribution only. Whereas the relative normalization changes as a function p_T^{min} by an order of magnitude for the exclusive BL model, it tends to be rather stable for the KMR model (the uncertainty on the factor 2.5 might be relatively large since we do not have a full simulation interface and the simulation effects tend to be higher at low jet transverse momentum). Finally, in Figs. 4 and 5, the fitted distributions are depicted for $p_T^{\text{min}} = 10, 25$ GeV jets, respectively.

The Tevatron data are well described by the combination of the FM and KMR models. We attribute the departure from the smooth distribution of the data to the imperfection of our fast simulation interface. On the contrary, the BPR model is disfavored because it fails to describe the low R_{JJ} region. It is because of the β_i factor in the parton density $f_{i/\mathbb{P}}(\beta_i)$ used by the BPR model (see footnote ¹ where the variables are defined) that the R_{JJ} distribution is shifted towards higher values. This factor was introduced to maintain the correspondence between the inclusive and exclusive models in the limit $f_{i/\mathbb{P}}(x_i) \rightarrow \delta(x_i)$. On the contrary, this assumption leads to properties in contradiction with CDF data. Using the BPR model without this additional normalization factor leads to a DMF which is in fair agreement with data. Indeed, we show in Fig. 6 the predictions of the “modified” model [i.e. defined as $f_{i/\mathbb{P}}(\beta_i) \equiv G_{i/\mathbb{P}}(\beta_i)$] for $p_T > 10$ GeV and $p_T > 25$ GeV jets. We see that the low R_{JJ} region is described well and that fitting the prediction of the exclusive KMR model with the BPR model yields roughly the same amount of exclusive events as using the factorable models. The BPR model will be revised to take these effects into account. We will not mention further this modified version of the BPR model since it gives similar results as the factorable models.

The exclusive BL model leads to a quite reasonable description of the DMF shape for both p_T^{min} cuts in combination with FM; however, it fails to grasp the shape of the exclusive cross section measured as a function of the jet minimal transverse momentum p_T^{min} . To illustrate this, we present the CDF data for the exclusive cross section corrected for detector effects compared with the predictions of both exclusive models after applying the same cuts as in the CDF measurement, namely, $p_T^{\text{jet}1,2} > p_T^{\text{min}}$, $|\eta^{\text{jet}1,2}| < 2.5$, $3.6 < \eta_{\text{gap}} < 5.9$, $0.03 < \xi_{\bar{p}} < 0.08$. As seen in Fig. 7, the BL exclusive model shows a much

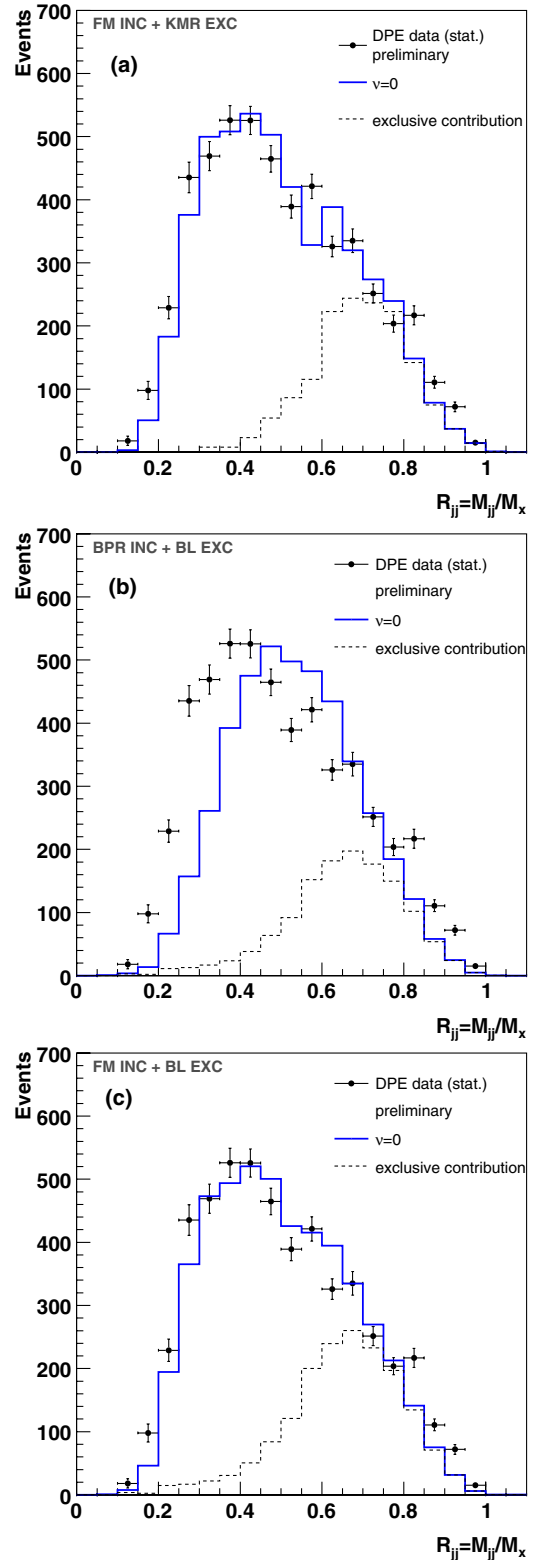


FIG. 4 (color online). Dijet mass fraction for jets $p_T > 10$ GeV. FM + KMR (a), BPR + BL (b), FM + BL (c) models. We notice that the exclusive contribution allows one to describe the tails at high R_{JJ} .

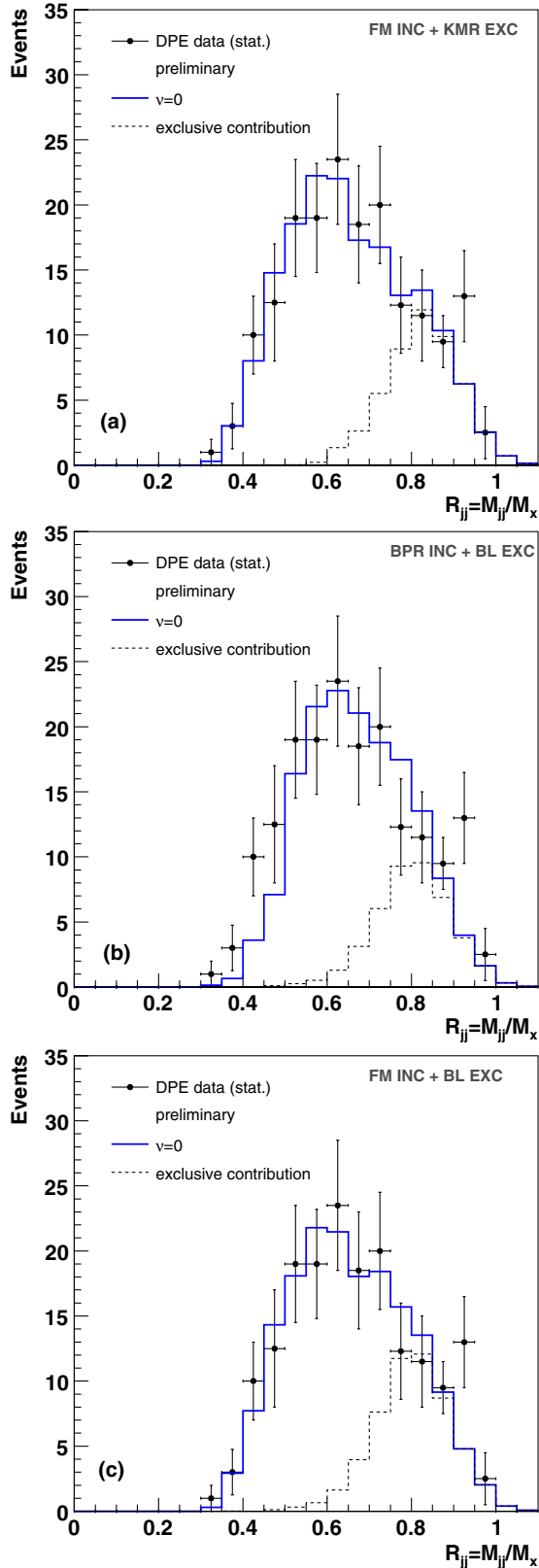


FIG. 5 (color online). Dijet mass fraction for jets $p_T > 25$ GeV. FM + KMR (a), BPR + BL (b), FM + BL (c) models. We note that the exclusive contribution allows one to describe the tails at high R_{JJ} .

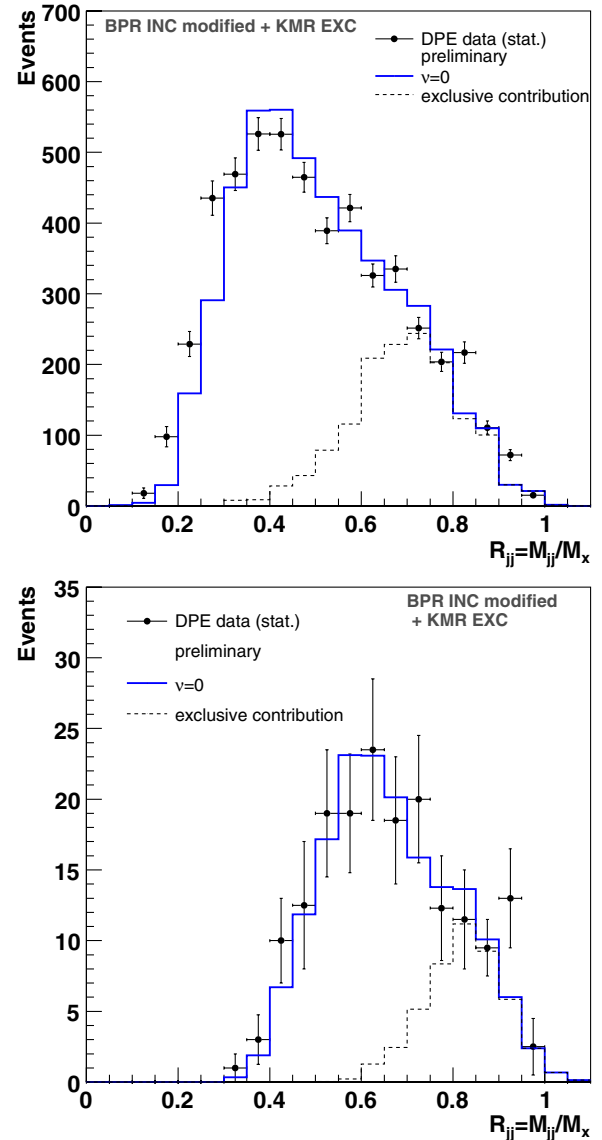


FIG. 6 (color online). Dijet mass distribution at the Tevatron calculated with the modified parton densities in the BPR model (see text) for 10 GeV (top panel) and 25 GeV (bottom panel) jets, KMR exclusive model included.

weaker p_T dependence than the KMR model and is in disagreement with data.²

To finish the discussion about the Pomeronlike models, it is worth mentioning that these results assume that the

²Let us note that the cross section of exclusive events measured by the CDF Collaboration is an indirect measurement since it was obtained by subtracting the inclusive contribution using an older version of the gluon density in the Pomeron measured at HERA. In that sense, the contribution of exclusive events using the newest gluon density from HERA might change those results. However, as we noticed, even modifying the gluon density greatly at high β by multiplying the gluon distribution by $(1 - \beta)^\nu$ does not change the amount of exclusive events by a large factor, and thus does not modify the indirect measurement performed by the CDF Collaboration much.

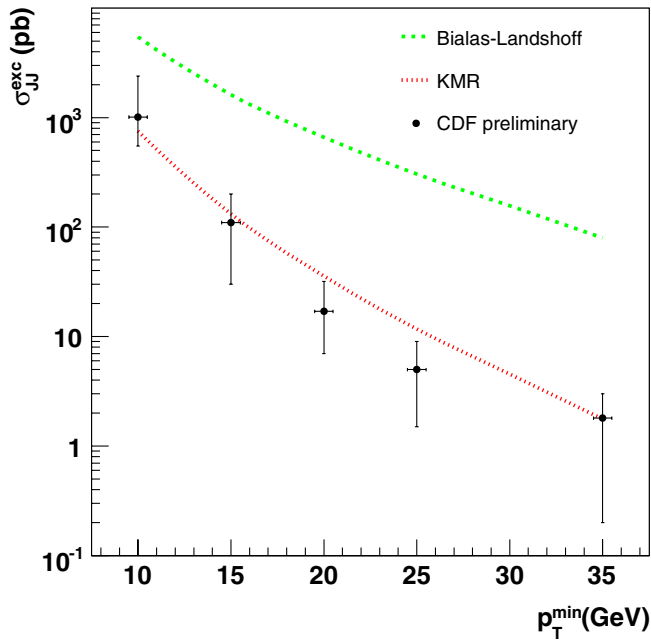


FIG. 7 (color online). Exclusive cross section as a function of the minimal transverse jet momentum p_T^{\min} measured by the CDF Collaboration and compared to the prediction of the KMR and BL exclusive models. We note that the BL model overshoots the CDF measurement while the KMR model is in good agreement.

survival probability has no strong dependence on β and ξ . If this is not the case, we cannot assume that the shape of the gluon distribution as measured at HERA could be used to make predictions at the Tevatron. However, this is a reasonable assumption since the survival probability is related to soft phenomena occurring during hadronization effects which occur at a much longer time scale than the hard interaction. In other words, it is natural to suppose that the soft phenomena will not be influenced by the hard interaction.

C. Prospects of future measurements at the Tevatron

In this section, we list some examples of observables which could be used to better identify the exclusive contribution in DMF measurements at the Tevatron. We present the prediction as a function of the minimal transverse momentum of the two leading jets p_T^{\min} . Since the BPR model does not describe the DMF at low R_{JJ} , we choose to show only the FM prediction in combination with both the KMR and BL exclusive models.

The same roman pot acceptance and restriction cuts as in the CDF measurement were used, specifically, $0.01 < \xi_{\bar{p}} < 0.12$, $p_T^{\text{jet}1,2} > p_T^{\min}$, $|\eta^{\text{jet}1,2}| < 2.5$, $3.6 < |\eta_{\text{gap}}| < 5.9$. Moreover, we adopted a normalization between inclusive and exclusive events as obtained for the $p_T > 25$ GeV analysis in the previous section, because we are less sensitive to the imperfections of the fast simulation interface for

higher p_T jets. Figure 8 illustrates the appearance of the DMF for two separate values of the minimum jet p_T^{\min} . The character of the distribution is clearly governed by exclusive events at high p_T^{\min} .

Figure 9 (top panel) shows the rate of DPE events. In addition to the curves denoting inclusive contribution with the varied gluon density for $\nu = -0.5, 0, 0.5$, the full contribution for both exclusive ν models is shown. For the FM model, which is in better consistency with accessible data, the measurement of the DPE rate does not provide an evident separation of exclusive contribution from the effects due to the Pomeron uncertainty since the noticeable difference appears when the cross sections are too low to be observable. It is possible, however, to examine the mean of the DMF distribution. As seen in Fig. 9 (bottom panel), this observable disentangles well the exclusive production with the highest effect between 30 and 40 GeV.

It needs to be stressed that, even though we obtain a hint in understanding the exclusive production phenomena at the Tevatron, the final picture cannot be drawn before precisely measuring the structure of the Pomeron. For this purpose, neither the DMF nor the DPE rate is suitable at the Tevatron. In the former, there is no sensitivity to the high β gluon variation, whereas in the latter, the gluon variation and the exclusive contribution cannot be easily separated. The way out is to perform QCD fits of the Pomeron structure in the gluon and the quark for data at low R_{JJ} where the exclusive contribution is negligible. Another possibility is to simultaneously perform the global fits of Pomeron structure functions using Dokshitzer-

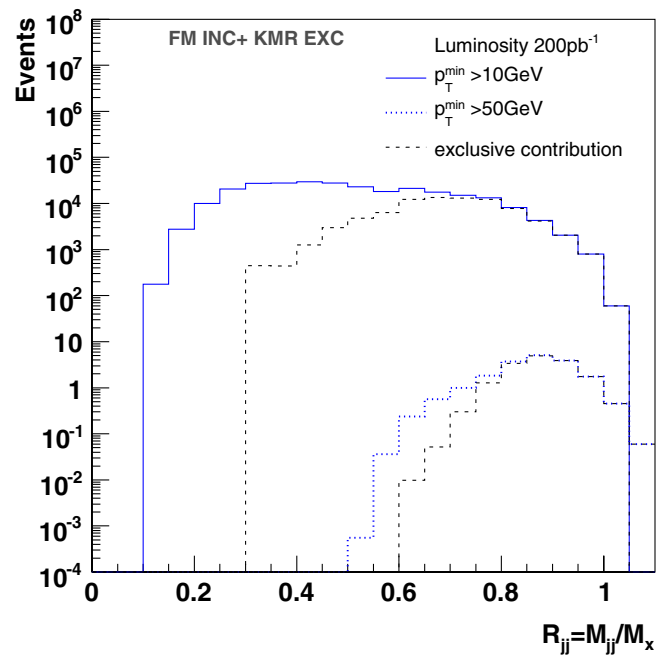


FIG. 8 (color online). Dijet mass fraction for two values of minimal transverse jet momentum p_T^{\min} . We note that the relative exclusive contribution is higher at high p_T^{\min} .

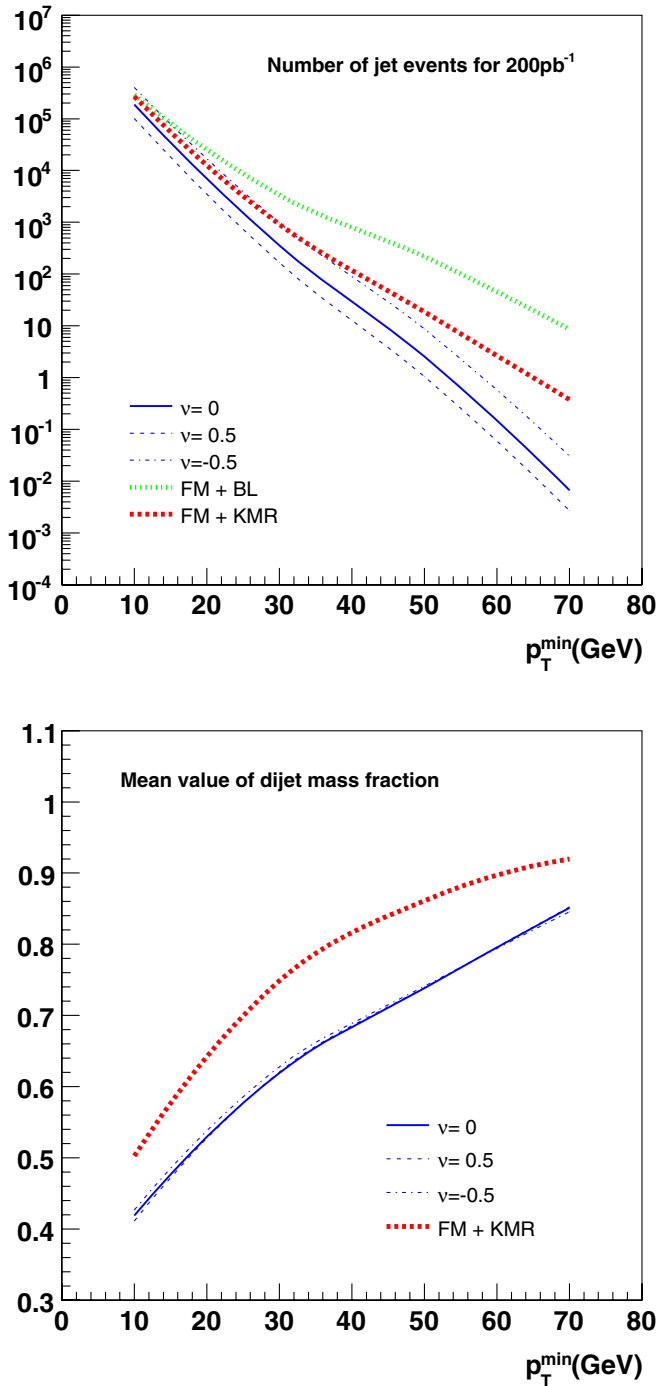


FIG. 9 (color online). Number of jet events and mean of the dijet mass fraction as a function of the minimal jet p_T^{\min} . We note that the ideal value of p_T^{\min} to enhance the exclusive contribution is of the order of 30–40 GeV which leads to a high enough production cross section as well as a large effect of the exclusive contribution on the dijet mass fraction.

Gribov-Lipatov-Altarelli-Parisi evolution and of the exclusive production.

A final important remark is that this study assumes Pomeronlike models for inclusive diffraction. It is worth

studying other models like soft color interaction processes and finding out if they also lead to the same conclusion concerning the existence of exclusive events.

D. Soft color interaction model

The soft color interaction model uses a different approach to explain diffractive events. In this model, diffraction is due to special color rearrangement in the final state as we mentioned earlier. It is worth noting that, in this model, the CDF data are dominated by events with a tagged antiproton on the \bar{p} ($\eta_{\bar{p}} < 0$) side and a rapidity gap on the p side. In other words, in most of the events, there is only one single antiproton in the final state accompanied by a bunch of particles (mainly pions) flowing into the beam pipe. This is illustrated in Fig. 10 (bottom panel)

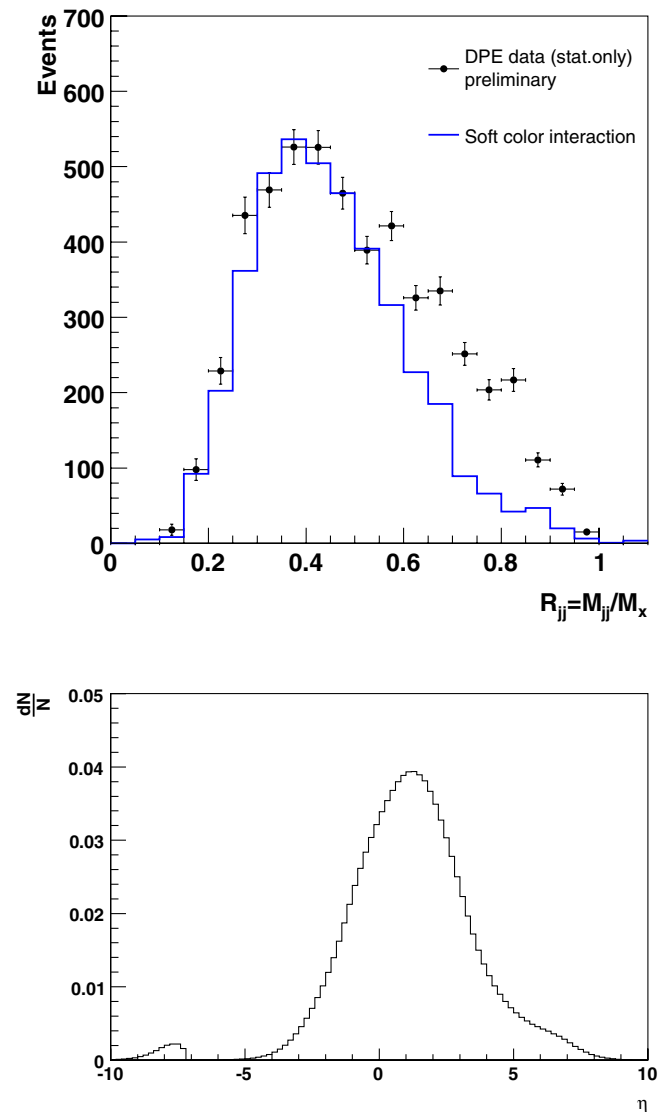


FIG. 10 (color online). Dijet mass fraction at the Tevatron for jets $p_T > 10$ GeV (top panel) and the η distribution of produced particles (bottom panel) for the soft color interaction model.

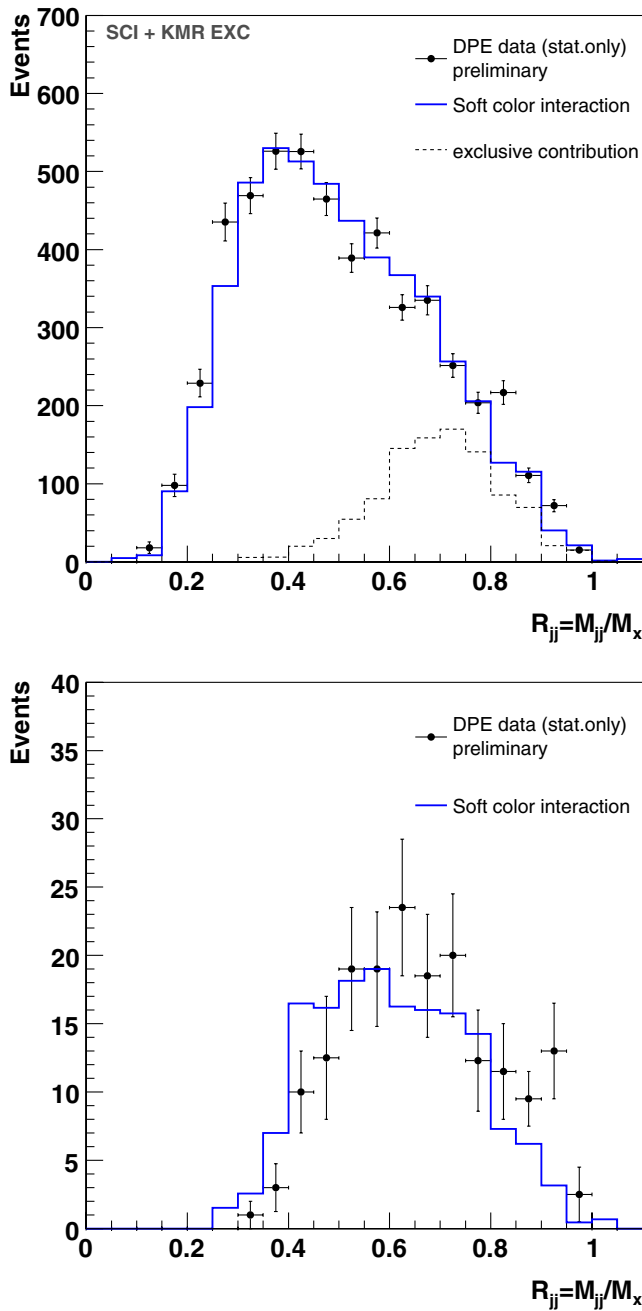


FIG. 11 (color online). Dijet mass fraction at the Tevatron for jets $p_T > 10$ GeV for the SCI model and the KMR exclusive model (top panel), and for jets $p_T > 25$ GeV for the SCI model only (bottom panel).

which shows the rapidity distribution of produced particles, and we notice the tail of the distribution at high rapidity. We should not neglect to mention that, on the other hand, the probability to get two protons intact (which is important for the double tagged events) is, in the SCI model, extremely small.

After applying all CDF cuts mentioned above, the comparison between SCI and CDF data on R_{JJ} is shown in

Fig. 10 (top panel) and Fig. 11. Whereas it is not possible to describe the full dijet mass fraction for a jet with $p_T > 10$ GeV, it is noticeable that the exclusive contribution is found to be lower than in the case of the Pomeron inspired models. Indeed, performing the same independent fit with the SCI model and the KMR exclusive contribution, one finds that only 70% of the exclusive contribution needed in the case of Pomeron inspired models is necessary to describe the data. For jets with $p_T > 25$ GeV, no additional exclusive contribution is needed to describe the measurement, which can be seen in Fig. 11. Since most events are asymmetric in the sense that only the antiproton is strictly intact and on the other side there is a flow of particles in the beam pipe, it is worth studying the rapidity distribution of jets for this model. The results are shown in Fig. 12. We note that the rapidity distribution is boosted towards high values of rapidity and not centered around zero like for Pomeron inspired models and CDF data. Moreover, the cross section for $p_T > 10$ GeV jets in the case of the SCI model is $\sigma^{\text{SCI}} = 167$ pb, only 13% of the cross section predicted by the Pomeron inspired models which, however, give a correct prediction of a large range of observables

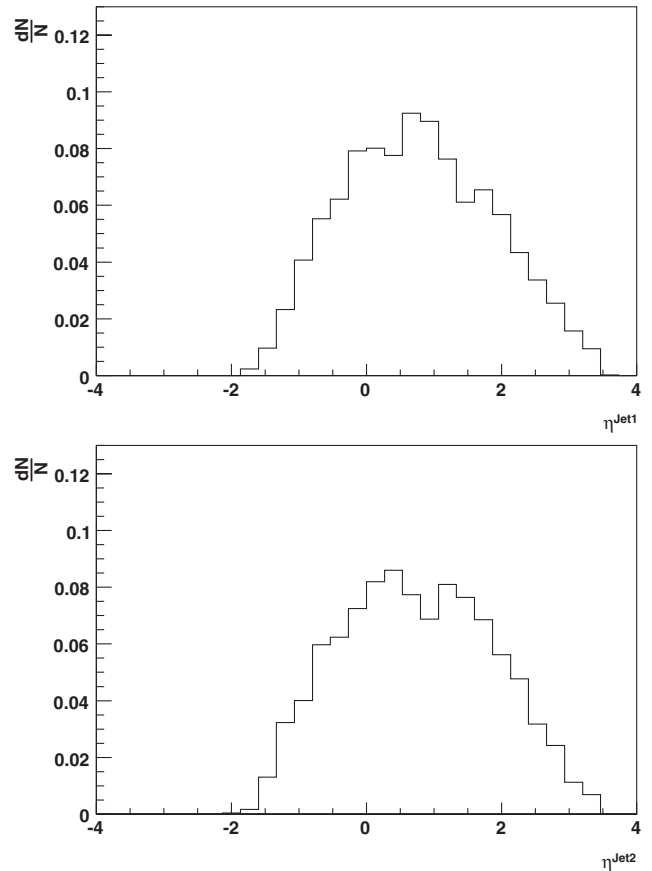


FIG. 12. Rapidity distribution of a leading jet (top panel) and a second leading jet (bottom panel) in the SCI model when calculating the dijet mass fraction.

including DPE cross sections. Therefore, such properties disfavor the SCI model. However, it would be worth studying and modifying the SCI model since the probability to observe two protons in the final state (and/or two gaps) should be higher than the square probability of observing one proton (and/or one gap) only (single diffraction), as was seen by the CDF Collaboration [20]. The reason that there are so few double proton events may have to do with the fact that the recombination of the color singlet system into a proton is quite sensitive to the details of the PYTHIA model for how the longitudinal momentum is shared in the proton remnants. This is not well constrained by data. The model needs to be tuned to take this into account, and then it would be interesting to see the impact on the dijet mass fraction and the existence of exclusive events.

IV. DIJET MASS FRACTION AT THE LHC

It was suggested that exclusive production at the LHC could be used to study the properties of a specific class of centrally produced objects like Higgs bosons. However, it relies on many subtleties such as a good understanding of the inclusive production. The perturbative nature of the diffractive processes results in the factorization of the cross section to a Regge flux and Pomeron structure functions, while factorization breaking appears via the survival probability only. The most important feature is the gluon density in the Pomeron, since its value at a high momentum fraction will control the background to exclusive DPE, and the Pomeron flux and the survival probability factor will have to be measured at the LHC to make reliable predictions.

The flux depends on the Pomeron intercept $\alpha_{\mathbb{P}}$ whose impact on the DMF distribution for LHC energies is shown in Fig. 13. The Pomeron intercept is parametrized as $\alpha_{\mathbb{P}} = 1 + \epsilon$, and the prediction is made for four values of $\epsilon = 0.5, 0.2, 0.12, 0.08$. The updated HERA Pomeron structure function analysis [13] suggests that the “hard Pomeron” intercept value is close to $\alpha_{\mathbb{P}} = 1.12$. Nevertheless, new QCD fits using single diffractive or double Pomeron exchange data will have to be performed to fully constrain the parton densities and the Pomeron flux at the LHC.

We also give the dependence of the DMF on jet p_T at the LHC. DPE events in this analysis were selected applying the roman pot acceptance on both sides from the interaction point, and using a fast simulation of the CMS detector [21] (the results would be similar using the ATLAS simulation) and requesting two leading jets with $p_T \geq 100, 200, 300, 400$ GeV. We have disfavored the predictions of the BL exclusive model at the Tevatron. The BL exclusive model shows weak p_T dependence which makes the model unphysical for LHC energies since it predicts cross sections even higher than the inclusive ones. We therefore focus on the predictions of FM and KMR models, only. As in the previous sections, we also include a study of the

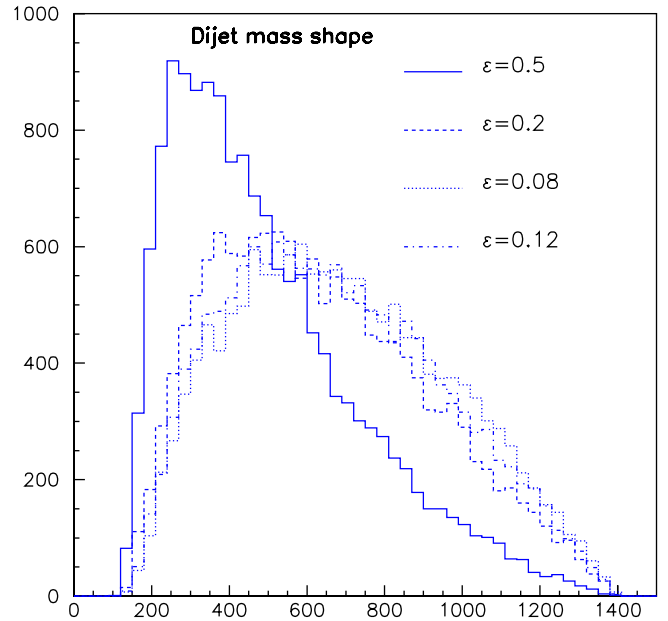


FIG. 13 (color online). Sensitivity of the dijet mass fraction to different values of the Pomeron intercept $\alpha_{\mathbb{P}} = 1 + \epsilon$.

uncertainty on the gluon density enhancing the high β gluon with a factor $(1 - \beta)^\nu$.

The dijet mass fraction as a function of different p_T is visible in Fig. 14. The exclusive contribution manifests itself as an increase in the tail of the distribution which can be seen for 200 GeV jets (top panel) and 400 GeV jets (bottom panel), respectively, in Fig. 15. Exclusive production slowly turns on with the increase of the jet p_T which is

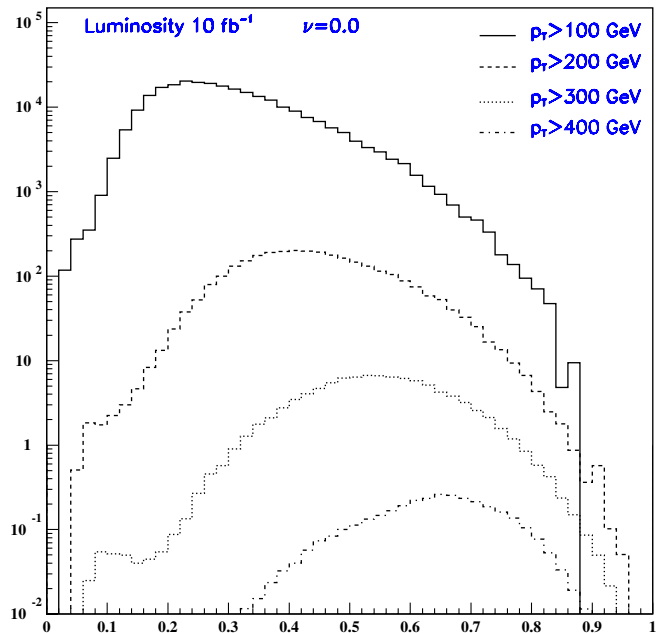


FIG. 14 (color online). Dijet mass fraction at the LHC as a function of jet minimal transverse momentum p_T^{\min} , FM inclusive model.

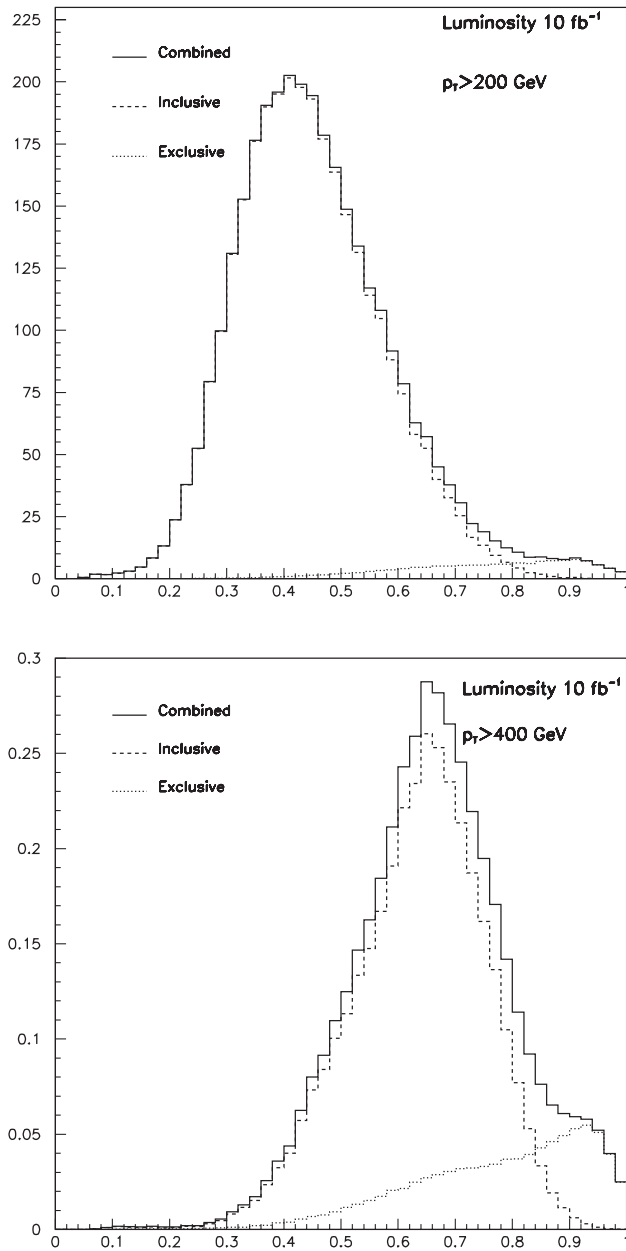


FIG. 15. Dijet mass fraction at the LHC for jets $p_T > 200$ GeV and $p_T > 400$ GeV, respectively, FM inclusive + KMR exclusive models.

demonstrated in Fig. 16 where the number of expected DPE events is shown. However, with respect to the uncertainty on the gluon density, this appearance is almost negligible. One can use the average position of the DMF as a function of the minimal jet transverse momentum p_T^{\min} to study the presence of the exclusive contribution; see Fig. 17. This is true especially for high p_T jets.

The exclusive production at the LHC plays a minor role for low p_T jets. Therefore, measurements e.g. for $p_T < 200$ GeV where the inclusive production is dominant could be used to constrain the gluon density in the Pomeron.

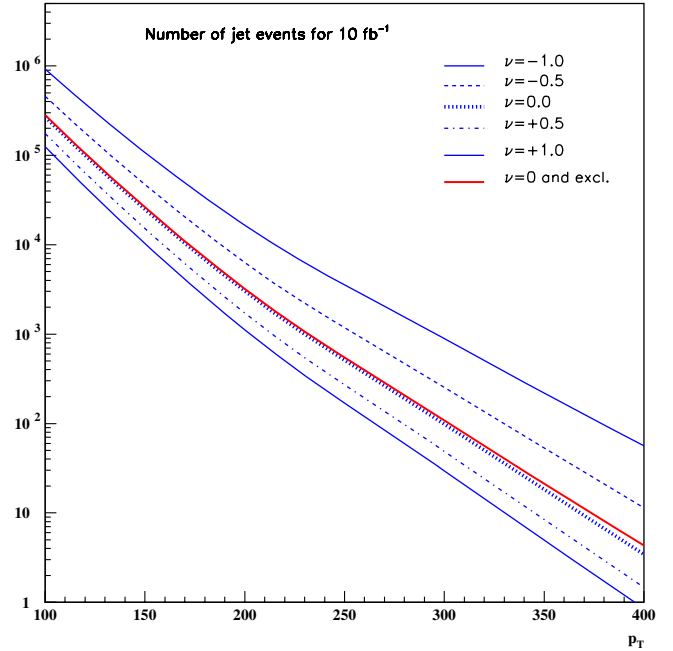


FIG. 16 (color online). Number of DPE events at the LHC as a function of minimal transverse momentum p_T^{\min} of two leading jets, FM inclusive + KMR exclusive models. The gluon variation is displayed for different ν values.

Afterwards, one can look in the high p_T jet region to extract the exclusive contribution from the tail of the DMF.

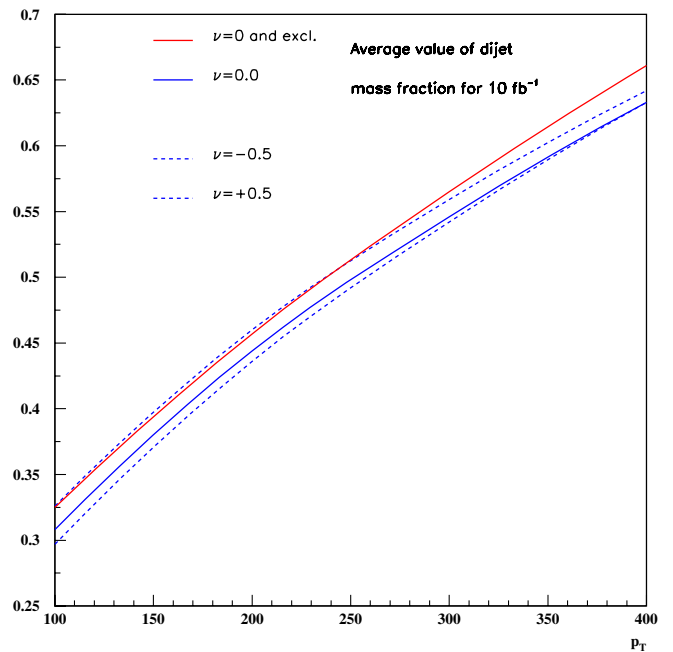


FIG. 17 (color online). Average value of the dijet mass fraction as a function of minimal transverse momentum p_T^{\min} of the leading jets, FM + KMR models. Exclusive contribution and different values of ν are shown.

V. CONCLUSION

The aim of this paper was to investigate whether we can explain the excess of events at the high dijet mass fraction measured at the Tevatron without the exclusive production. The result is actually twofold.

Concerning the Pomeron induced models (“factorized model” and Bialas-Landshoff inclusive models) we found that the uncertainty on the high β gluon density in the Pomeron has a small impact at high R_{JJ} . Therefore, an additional contribution is needed to describe the CDF data with these models. We examined the exclusive KMR model and Bialas-Landshoff exclusive model predictions for the role of the additional contribution and found that the best description of data is achieved by the combination of the factorized inclusive model (or the modified inclusive Bialas-Landshoff one) and the KMR exclusive model. The exclusive contribution at the Tevatron can be magnified requesting higher p_T jets and studying specific observables like a mean of the dijet mass fraction, for example. However, one of the limitations of using high p_T jets is due to the rate of DPE events which falls logarithmically, allowing measurements for jets up to approximately 40 GeV. The Bialas-Landshoff exclusive model seems to be disfavored by Tevatron data since it shows a softer jet p_T dependence and predicts unphysically large DPE rates at LHC energies.

In the case of the soft color interaction model which is not based on Pomeron exchanges, the need to introduce an additional exclusive production is less obvious. For low p_T jets the amount of exclusive events to describe the data is smaller than in the case of the factorized model, but for

high p_T jets no additional contribution is necessary. This draws a new question: Can the double Pomeron exchange events be explained by a special rearrangement of color only? The CDF data are, in this model, dominated by single diffractive events. The probability of tagging two protons in the final state within this model is very small, contradicting the CDF observation. So even though the SCI model is not applicable for DPE events in the current state, it would be worth adjusting this model to correctly predict the rate of double tagged events and to study the model prediction of the dijet mass fraction and other DPE induced processes.

The dijet mass fraction at the LHC could be used to select the exclusive events. Indeed, it is possible to study jets with $p_T > 200$ GeV, for instance, and to focus on events with the DMF above 0.8 which is dominated by exclusive production (see Fig. 15). However, as it was advocated earlier, a complete QCD analysis consisting of measuring the gluon density in the Pomeron (especially at high β) and studying the QCD evolution of exclusive events as a function of jet p_T is needed to fully understand the observables, and to make predictions for diffractive Higgs production and its background at the LHC as an example.

ACKNOWLEDGMENTS

The authors want to thank M. Boonekamp, R. Enberg, D. Goulianos, G. Ingelman, R. Pechanski, and K. Tereashi for useful discussions and for providing them with the CDF data and roman pot acceptance.

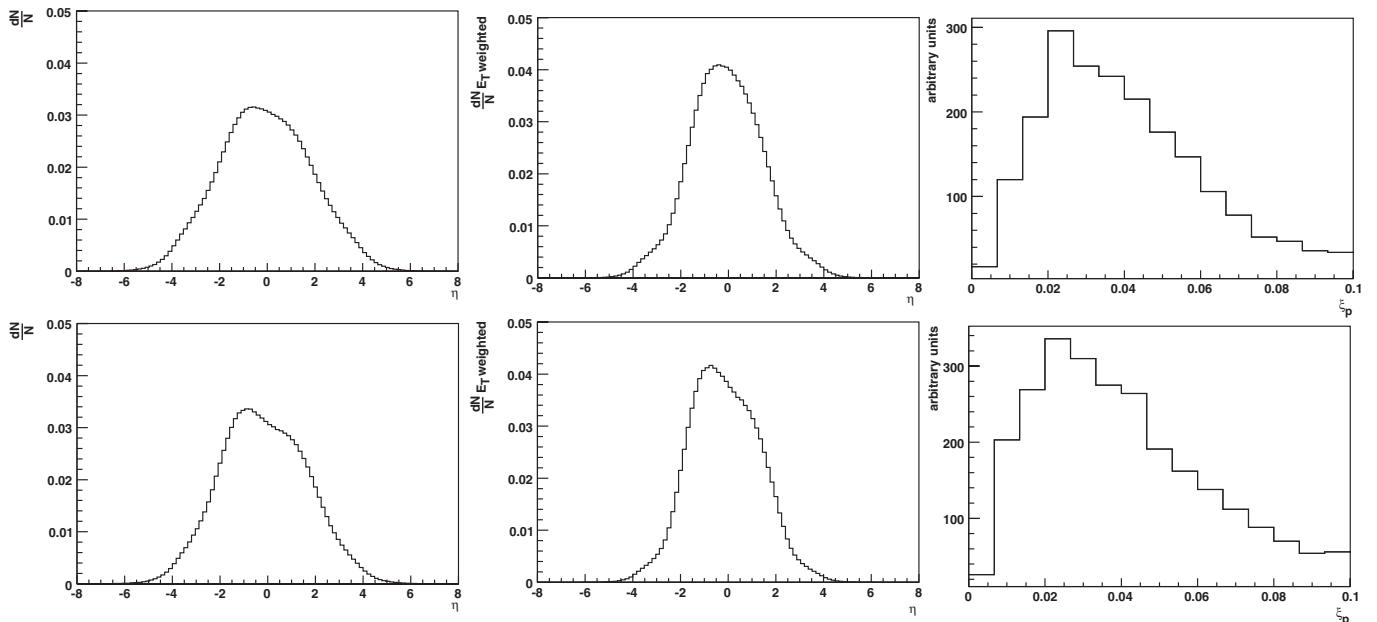


FIG. 18. Left and middle plots: Rapidity and E_T weighted rapidity distributions of all particles produced (except the protons); right plots: momentum loss of the proton in double Pomeron exchange events ξ_p for FM (top plot) and BPR (bottom plot) inclusive models.

APPENDIX

Throughout the paper, we have purposely omitted a discussion of imperfections concerning the dijet mass fraction reconstruction within our framework, postponing it to this section. In this appendix, all calculations are done for jets with $p_T > 10$ GeV.

- (i) In our analysis, we defined the dijet mass fraction as a ratio of the two leading jet invariant mass M_{JJ} to the central diffractive mass M_X . The latter was determined using the momentum loss $\xi_{\bar{p}}$ measured in a roman pot on the antiproton side and the ξ_p^{part} obtained from particles on the generator level, such as $M_X = (s\xi_{\bar{p}}\xi_p^{\text{part}})^{1/2}$. In this case, we must ensure that all of the produced diffractive energy M_X is deposited into the central detector. If this is not the case, our M_X at generator level might be sensibly larger than the one measured by the CDF Collaboration. The energy flow of the particles on the generator level as a function of rapidity is shown in Fig. 18, upper plot. The middle plot shows the energy flow

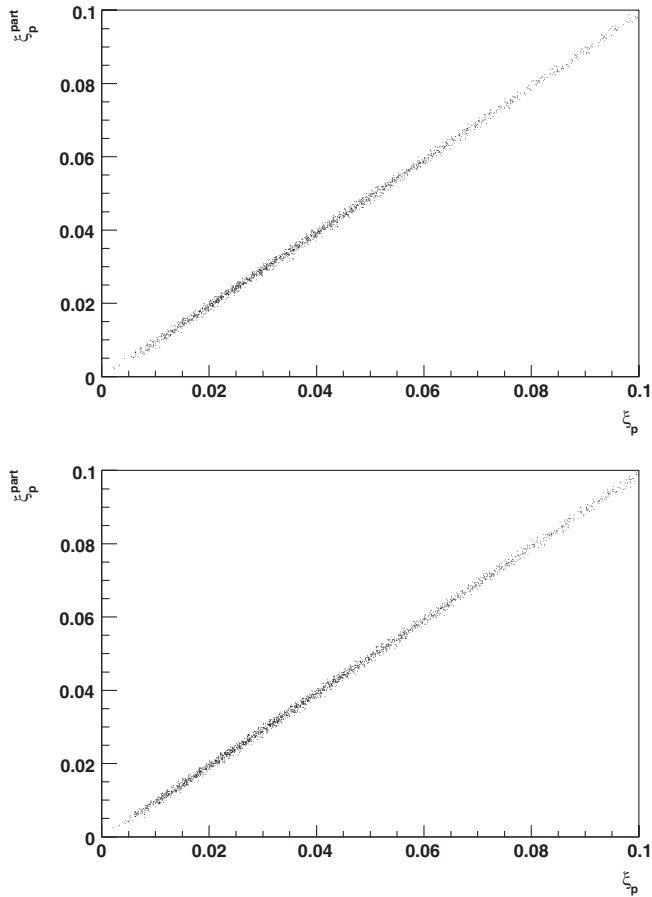


FIG. 19. Comparison of the proton momentum loss ξ_p^{part} calculated with formula (2) and the proton momentum loss ξ_p^{cr} at generator level for FM (top panel) and BPR (bottom panel) models.

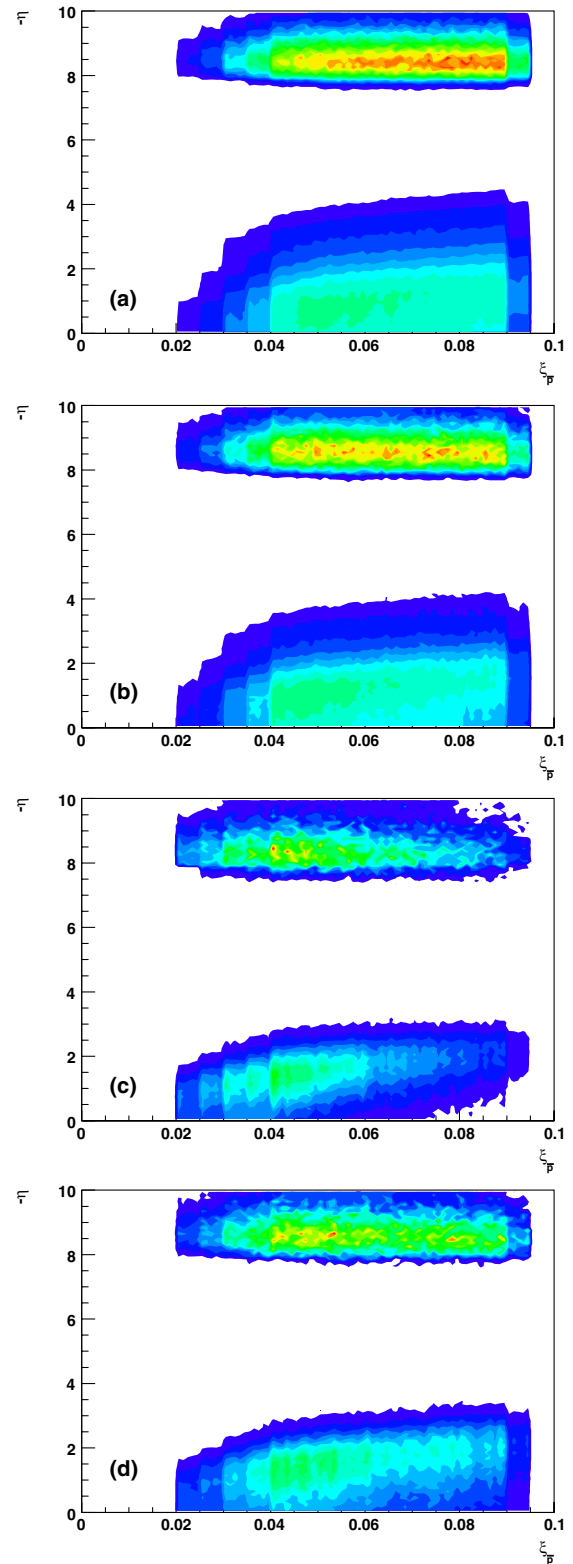


FIG. 20 (color online). Rapidity of particles on the \bar{p} side vs \bar{p} momentum loss: inclusive models for FM (a) and BPR (b); exclusive models for KMR (c) and BL (d). Hits of scattered \bar{p} are included.

weighted by the transverse momentum of the particle E_T . We see that most of the energy is deposited in the calorimeter region, i.e. for $|\eta| < 4$. In \bar{p} tagged events, protons most frequently lose a smaller momentum fraction (roughly $\xi_p \sim 0.025$) than the tagged antiproton for which the acceptance turns on for $\xi_{\bar{p}} > 0.035$. This can be seen from the ξ_p population plot on the right of Fig. 18. Thus, a

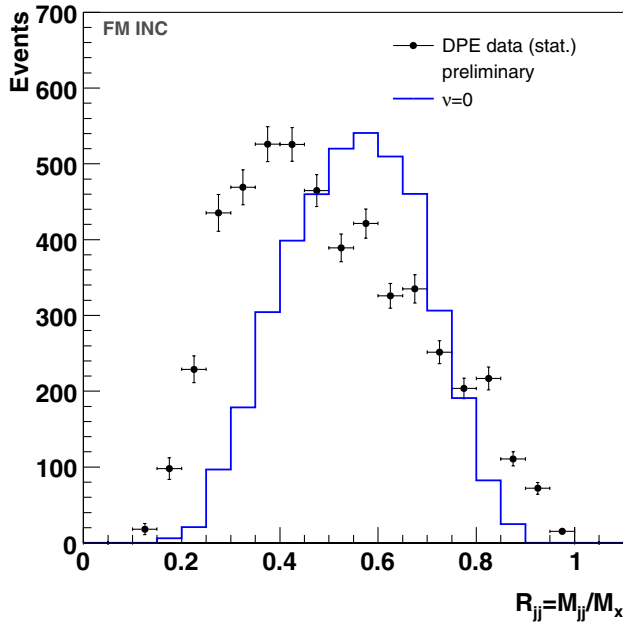
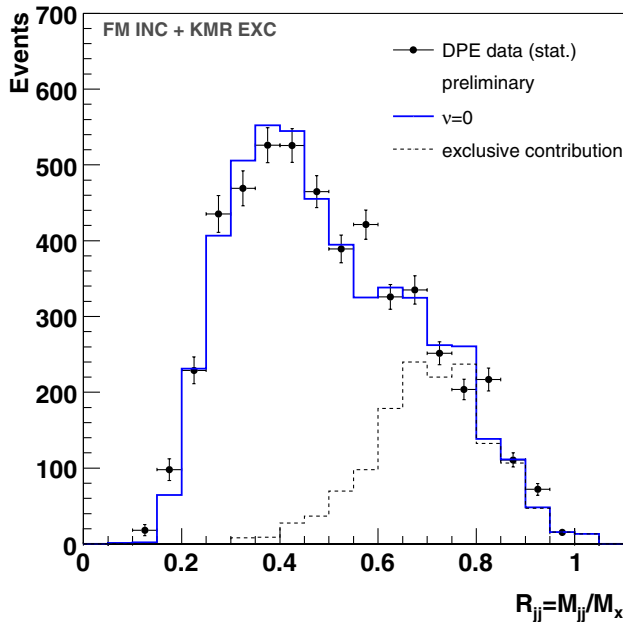


FIG. 21 (color online). Dijet mass fraction for jets $p_T > 10$ GeV: FM + KMR (top panel), and at generator level calculated according to (A2) (bottom panel).

collision of a more energetic Pomeron from the antiproton side with a Pomeron from the proton side is boosted towards the \bar{p} , as is seen on the energy flow distributions.

- (ii) A comparison between the proton momentum loss obtained from particles ξ_p^{part} calculated using formula (2) and the proton momentum loss at generator level ξ_p leads to the factor 1.1 mentioned in a previous section. The dependence is displayed in Fig. 19.
- (iii) The size of the rapidity gap runs as a function of the momentum loss ξ like $\Delta\eta \sim \log 1/\xi$. The size of the gap which increases with decreasing ξ for inclusive models can be seen in Fig. 20. Regions of high rapidity show the \bar{p} hits, whereas the low rapidity region is due to the produced particles detected in the central detector; they are well separated by a rapidity gap. For exclusive events, the size of a rapidity gap is larger and does not show such a strong ξ dependence as for inclusive models.
- (iv) The simulation interface plays a significant role in the determination of the exclusive contribution. As previously stated, we cannot profit from having access to the full simulation interface and having under control all the effects of the detector. In order to eliminate some effects of the simulation we plot the dijet mass distribution R_{JJ} using the information from the generator and check whether the need for

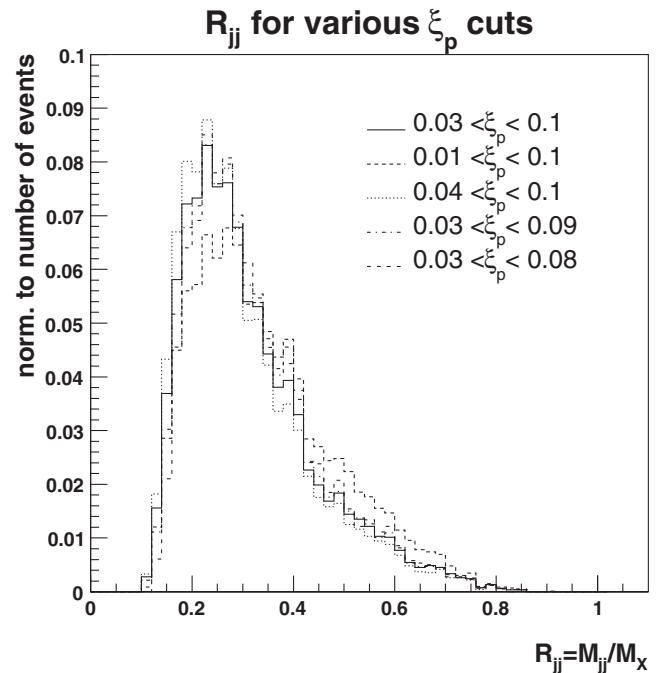


FIG. 22. Dijet mass fraction on the generator level for $p_T^{\text{parton}1,2} > 10$ GeV, $0.03 < \xi_{\bar{p}} < 0.095$, and ξ_p cut as specified in the figure. The shape of the DMF is less sensitive to the actual ξ_p cut. See the discussion in Sec. III A for details.

exclusive events to describe the data is still valid. Specifically, we require the same cuts as in Sec. III but the diffractive mass M_X^{RP} is evaluated using the true (anti)proton momentum loss $(\xi_{\bar{p}})\xi_p$ at generator level,

$$M_X^{RP} = \sqrt{s\xi_{\bar{p}}\xi_p}. \quad (\text{A1})$$

The dijet mass fraction calculated with M_X^{RP} is shown in Fig. 21. We see that the distribution is shifted to lower values of R_{JJ} , requesting slightly more exclusive events to describe the CDF data. The description of the data is also quite good.

(v) The role of the simulation interface to reconstruct

jets can be illustrated by comparing the above distributions to the DMF calculated at generator level defined as

$$R_{JJ} = \frac{M_{JJ}}{M_X} = \frac{\sqrt{s\xi_{\bar{p}}\xi_p\beta_1\beta_2}}{\sqrt{s\xi_{\bar{p}}\xi_p}} = \sqrt{\beta_1\beta_2}, \quad (\text{A2})$$

where β_1, β_2 denote the fraction of the Pomeron carried by the interacting parton. As can be seen in Fig. 21 (bottom panel), the DMF distribution at pure generator level shows a completely different shape not compatible with CDF data and it shows the importance of jet reconstruction.

-
- [1] M. Boonekamp, R. Peschanski, and C. Royon, Phys. Lett. B **598**, 243 (2004).
- [2] C. Royon, Mod. Phys. Lett. A **18**, 2169 (2003).
- [3] M. Boonekamp, A. De Roeck, R. Peschanski, and C. Royon, Acta Phys. Pol. B **33**, 3485 (2002); Phys. Lett. B **550**, 93 (2002).
- [4] M. Boonekamp, J. Cammin, S. Lavignac, R. Peschanski, and C. Royon, Phys. Rev. D **73**, 115011 (2006).
- [5] B. Cox, J. Forshaw, and B. Heinemann, Phys. Lett. B **540**, 263 (2002).
- [6] V. A. Khoze, A. D. Martin, and M. G. Ryskin, Phys. Lett. B **650**, 41 (2007).
- [7] V. A. Khoze, A. D. Martin, and M. G. Ryskin, Eur. Phys. J. C **48**, 467 (2006).
- [8] M. Boonekamp, R. Peschanski, and C. Royon, Phys. Rev. Lett. **87**, 251806 (2001); Nucl. Phys. **B669**, 277 (2003); **B676**, 493 (2004).
- [9] M. Boonekamp and T. Kucs, Comput. Phys. Commun. **167**, 217 (2005).
- [10] We used the PYTHIA SCI MONTE CARLO program described in <http://www.isv.uu.se/thepp/MC/scigal/>.
- [11] G. Ingelman and P. E. Schlein, Phys. Lett. **152B**, 256 (1985).
- [12] A. A. Affolder *et al.* (CDF Collaboration), Phys. Rev. Lett. **84**, 5043 (2000).
- [13] C. Royon, L. Schoeffel, S. Sapeta, R. Peschanski, and E. Sauvan, arXiv:hep-ph/0609291.
- [14] A. Bialas and P. V. Landshoff, Phys. Lett. B **256**, 540 (1991); A. Bialas and W. Szeremeta, Phys. Lett. B **296**, 191 (1992); A. Bialas and R. Janik, Z. Phys. C **62**, 487 (1994).
- [15] A. Bzdak, Acta Phys. Pol. B **35**, 1733 (2004).
- [16] V. A. Khoze, A. D. Martin, and M. G. Ryskin, Eur. Phys. J. C **19**, 477 (2001); **20**, 599 (2001); **23**, 311 (2002); **24**, 581 (2002).
- [17] A. Edin, G. Ingelman, and J. Rathsman, Z. Phys. C **75**, 57 (1997); R. Enberg, G. Ingelman, A. Kissavos, and N. Timneanu, Phys. Rev. Lett. **89**, 081801 (2002).
- [18] CDF Collaboration, CDF note 8493 (2006).
- [19] Fast simulation of the CDF and D0 detectors, SHW package.
- [20] D. Acosta *et al.* (CDF Collaboration and CDFII Collaboration), Phys. Rev. Lett. **91**, 011802 (2003).
- [21] CMSIM, fast simulation of the CMS detector, CMS Collaboration, Technical Design Report 1997; TOTEM Collaboration, Technical Design Report, CERN/LHCC/99-7; ATLFAST, fast simulation of the ATLAS detector, ATLAS Collaboration, Technical Design Report, CERN/LHC C/99-14.